Effects of Small Vibrations on The Surface of a Liquid Bridge

By
R.Q. Liang and M. Kawaji

Abstract: The effects of small vibrations on the surface oscillation of a liquid bridge, especially the resonance behavior, were investigated numerically, using a three-dimensional code based on the level set method to capture the gas-liquid interface. The surface oscillation of an isothermal liquid bridge held vertically between solid disks was predicted, and the predictions were compared with an analytical model based on a mass-spring-damper analogy. By subjecting the liquid bridge to various horizontal vibrations, the surface resonance frequencies were clearly determined numerically and analytically. The numerical resonance frequencies compared well with the analytical model predictions. The effect of small vibrations on the surface oscillation amplitudes of the liquid bridge was also investigated.

1. INTRODUCTION

In preparation for a Marangoni convection experiment proposed in an International AO and to be conducted aboard the International Space Station using the Fluid Physics Experiment Facility (FEPF) in JEM, it is necessary to investigate the g-jitter induced oscillation of a liquid bridge surface. The liquid bridge in the IAO experiment simulates a floating zone method which is a popular technique used to produce single crystals of semiconductor materials. In this method, a solid rod is heated from outside to melt a part of the rod so that the molten material is held between two solid rods. By gradually moving the heated zone, the molten zone also moves leaving behind a crystal structure in the solidified zone. When the floating zone method is used in space, two effects have been identified which may produce fluid motion within the liquid bridge:

1. Marangoni convection due to a temperature and/or concentration gradient at the liquid surface,
2. Small accelerations referred to as g-jitter due to small vibrations.

Many investigations into Marangoni flow in the liquid bridge have shown that the Marangoni flow changes from a steady to oscillatory flow when the temperature and/or concentration gradient exceeds a critical value [1-7]. Such an oscillation in flow may lead to non-uniformities in crystal structure such as striations.

Apart from the effect of Marangoni convection, the behavior of the liquid bridge may also be affected significantly by small vibrations in space platforms such as the International Space Station. These vibrations are caused by the operation of various on-board devices, physical activities of astronauts, thruster firings for attitude control and so on. Since g-jitter is known to contain a wide spectrum of vibration frequencies and the liquid bridge may have one or more resonance frequencies, its free surface may oscillate dynamically with very high amplitudes, even though the vibration amplitude is very small. The dynamic oscillations of the free surface may in turn affect the oscillatory Marangoni convection phenomnena.

In order to predict the dynamic response of a liquid bridge to small vibrations under microgravity conditions, numerical and analytical models were developed. A three-dimensional numerical simulation model uses a DNS technique coupled with a level set approach to capture the interface motions of small amplitudes for non-

Department of Chemical Engineering and Applied Chemistry, University of Toronto, 200 College Street, Toronto, Ontario M5S 3E5, Canada

axisymmetric, viscous and isothermal liquid bridges. An analytical model had also been developed to predict the resonance behavior of a cylindrical liquid bridge subjected to horizontal vibrations. The model contained one adjustable parameter, the value of which has been determined in this work by comparing the predictions of the numerical and analytical models. The numerical model was then used to determine the vibration characteristics of liquid bridges of large diameter (D = 30 mm) and height (H = 10) under microgravity, subjected to single-frequency vibration normal to the liquid bridge axis.

2. NUMERICAL MODEL FORMULATION

2.1 EQUATIONS OF MOTION

The equations of motion for an incompressible flow are given by the following Navier-Stokes equations which include gravitational and small horizontal acceleration forces, and viscosity and surface tension effects.

$$\frac{\partial u}{\partial x}+\frac{\partial v}{\partial y}+\frac{\partial w}{\partial z}=0, \tag{1}$$

$$\frac{\partial u}{\partial t}=-u\frac{\partial u}{\partial x}-v\frac{\partial u}{\partial y}-w\frac{\partial u}{\partial z}+FGX+\frac{1}{\rho}\left(-\frac{\partial p}{\partial x}+\frac{\mu}{\mathrm{Re}}\left(\frac{\partial^2 u}{\partial x^2}+\frac{\partial^2 u}{\partial y^2}+\frac{\partial^2 u}{\partial z^2}\right)+\frac{1}{We}\kappa\delta(d)\mathbf{n}\right), \tag{2}$$

$$\frac{\partial v}{\partial t}=-u\frac{\partial v}{\partial x}-v\frac{\partial v}{\partial y}-w\frac{\partial v}{\partial z}+\frac{1}{\rho}\left(-\frac{\partial p}{\partial y}+\frac{\mu}{\mathrm{Re}}\left(\frac{\partial^2 v}{\partial x^2}+\frac{\partial^2 v}{\partial y^2}+\frac{\partial^2 v}{\partial z^2}\right)+\frac{1}{We}\kappa\delta(d)\mathbf{n}\right), \tag{3}$$

$$\frac{\partial w}{\partial t}=-u\frac{\partial w}{\partial x}-v\frac{\partial w}{\partial y}-w\frac{\partial w}{\partial z}+\frac{1}{Fr^2}+\frac{1}{\rho}\left(-\frac{\partial p}{\partial z}+\frac{\mu}{\mathrm{Re}}\left(\frac{\partial^2 w}{\partial x^2}+\frac{\partial^2 w}{\partial y^2}+\frac{\partial^2 w}{\partial z^2}\right)+\frac{1}{We}\kappa\delta(d)\mathbf{n}\right). \tag{4}$$

Here, $FGX=\frac{g_x\bar{L}}{U_\infty^2}$ is the body force in x direction induced by external acceleration, $g_x=A\omega^2\sin\omega t$ is the external acceleration in x direction, A is the vibration amplitude, $\omega=2\pi f$ is the angular frequency and f is the vibration frequency, u, v, and w are the fluid velocities in x, y, and z directions, respectively, $\rho=\rho(\mathbf{x}, t)$ is the fluid density, $\mu=\mu(\mathbf{x}, t)$ is the fluid viscosity, κ is the curvature of the interface, d is the normal distance to the interface, δ is the Dirac delta function, $\mathbf{n}$ is the unit normal vector at the interface, t is the time, and p is the pressure.

The dimensionless parameters used are Reynolds number, Froude number, and Weber number defined as $\mathrm{Re}=\frac{\rho_l\bar{L}U_\infty}{\mu_l}$, $Fr=U_\infty\sqrt{\frac{1}{g\bar{L}}}$, $We=\frac{\rho_l\bar{L}U_\infty^2}{\sigma}$, respectively, where ρ_l and μ_l are the liquid density and viscosity, respectively and g is the gravitational acceleration.

2.2 Level set function and its formulation

The level set method was originally introduced by Osher and Sethian [8] to numerically predict the moving interface between two fluids. Instead of explicitly tracking the interface, the level set method implicitly captures the interface by introducing a smooth signed distance from the interface in the entire computational domain. The level set function is taken to be positive outside the liquid bridge, zero at the interface and negative inside the liquid bridge. We consider a closed moving interface $\Gamma(t)$, that encloses a region $\Omega(t)$. We associate $\Omega(t)$ with an auxiliary function $\phi(\mathbf{x}, t)$, which is called the level set function,

$$\phi(\mathbf{x},t)=\begin{cases}dist(\mathbf{x},\Gamma(t),t) & if\ \mathbf{x}\ outside\ \Gamma(t)\\ -dist(\mathbf{x},\Gamma(t),t) & if\ \mathbf{x}\ inside\ \Gamma(t)\end{cases}, \tag{5}$$

$$\Gamma(t)=\left\{\mathbf{x}\in\Omega:\phi(\mathbf{x},t)=0\right\}. \tag{6}$$

The density ρ and viscosity μ in the flow field can then be expressed as follows.

$$\rho(\phi)=\rho_{in}+(\rho_{out}-\rho_{in})H_\alpha(\phi), \tag{7}$$

$$\mu(\phi)=\mu_{in}+(\mu_{out}-\mu_{in})H_\alpha(\phi), \tag{8}$$

$$H_\alpha(\phi)=\begin{cases}0 & \phi<-\alpha \\ (\phi+\alpha)/(2\alpha)+\sin(\pi\phi/\alpha)/2\pi & |\phi|\le\alpha \\ 1 & \phi>\alpha\end{cases}, \tag{9}$$

where the suffixes *in* and *out* stand for the liquid and gas phases, respectively, and α is the prescribed thickness of the interface. In this work, we used α = x/2.

The interface motion is predicted by solving the following convection equation for the level set function ϕ given by,

$$\phi_t+\mathbf{u}\cdot\nabla\phi=0. \tag{10}$$

The 3-D problem was solved in the following computational domain,

$$\Omega=\left\{(x,y,z)\middle|\ 0\le x\le 4R,\ \ 0\le y\le 4R,\ \ 0\le z\le R\right\},$$

where R is the radius of the liquid bridge at the top and bottom. The non-slip condition was used at the upper and lower walls in contact with the liquid bridge, and the free-slip condition was used at the other wall boundaries.

2.3 Re-initialization of level set function

Because we initialize the level set function ϕ as a signed distance from the interface, we have

$$|\nabla\phi|=1. \tag{11}$$

When we move the level set function ϕ with Eq. (10), ϕ will no longer be a distance function and may become irregular at later times.

$$|\nabla\phi|\neq 1. \tag{12}$$

This will necessarily result in the variation of the interface thickness in time, making further computation and contour plotting highly inaccurate. Fortunately, we can ignore all values of ϕ far from the zero level set and replace the solution ϕ at any time by another function ϕ_0 with the same zero set as ϕ and then take ϕ_0 as the initial data to use. Sussman et al.'s [9] proposal for an iterative procedure is used to fulfill the above process.

$$\phi_t=sign(\phi_0)(1-|\nabla\phi|), \tag{13}$$

$$\phi(\mathrm{x},0)=\phi_0(\mathrm{x}). \tag{14}$$

2.4 Body force due to surface tension force

The model of Continuum Surface Force (CSF) was employed to treat the surface tension force at an interface, which interprets the surface tension force as a continuous effect across the interface rather than as a boundary condition on the interface [10]. By using the level set function, body force due to surface tension can be expressed as,

$$\frac{1}{We}\kappa\delta(d)\mathbf{n}=\frac{1}{We}\kappa(\phi)\delta(\phi)\nabla\phi. \tag{15}$$

The curvature of the interface is evaluated from

$$\kappa(\phi)=-(\nabla\cdot\mathbf{n})=-\nabla\cdot\left(\frac{\nabla\phi}{|\nabla\phi|}\right). \tag{16}$$

The Dirac delta function is defined as

$$\delta_\alpha(\phi)=\frac{dH_\alpha(\phi)}{d\phi}=\begin{cases}0 & |\phi|>\alpha \\ \dfrac{1}{2\alpha}\left[1+\cos\left(\dfrac{\pi\phi}{\alpha}\right)\right] & |\phi|\le\alpha\end{cases}. \tag{17}$$

2.5 Poisson equation solver

Briefly, we may write the Poisson equations for pressure as

$$\nabla \cdot \left(\frac{\nabla p}{\rho} \right) = \frac{\nabla \mathbf{G}}{\Delta t}, \tag{18}$$

$$\mathbf{G} = \begin{pmatrix} G_x \\ G_y \\ G_z \end{pmatrix} = \mathbf{u} + \Delta t \left(-(\mathbf{u}\cdot\nabla)\mathbf{u} + \frac{\mathbf{n}_{i\{i=x,z\}}}{Fr^2_{i\{i=x,z\}}} + \frac{1}{\rho}\left(\frac{1}{\mathrm{Re}} \nabla\cdot(2\mu D) + \frac{1}{We}\kappa(\phi)\delta(\phi)\nabla\phi \right) \right), \tag{19}$$

where $\mathbf{n}_{i(i=x,z)}$ is a unit normal vector in x or z direction.

The Successive Over Relaxation (SOR) method has been used to solve the Poisson equation for pressure.

2.6 The algorithm to catch small displacements of the surface

When a small vibration is applied, the movement of the liquid bridge surface can be extremely small, in the order of microns. It is not easy to capture such tiny surface movements in gas-liquid two phase flow simulations using grids of much larger dimensions. The Volume of Fluid method would have an insurmountable difficulty in overcoming this spatial resolution problem. In contrast, the level set approach can avoid this problem using a new algorithm developed in this work.

Step 1. Determine a monitoring point on the interface.

Step 2. Find out the grid point, which bounds the monitoring point outside the interface or on the interface when the interface moves through the grid at every time step.

Step 3. Calculate the position of the monitoring point.

Let us take a cross section in the x-y plane at a certain height of the liquid bridge. When the interface traverses through the grid, there are two ways for the interface to intersect with the grid. One way is that the interface intersects with the grid line between two grid points as shown in Fig. 1, and the other is the interface directly falling on one of the grid points. In Fig. 1, Γ represents the interface, and (i, j, k) and $(i+1, j, k)$ represent two arbitrary grid points on opposite sides of the interface (Γ). The level set function ϕ can be constructed by choosing the sign of ϕ to be negative inside the interface and positive outside the interface. If the interface intersects with the grid point, for example, (i, j, k), the level set function ϕ at this point should be zero and the position of the monitoring point in the x direction can be determined by using the coordinate value of (i, j, k). If the interface intersects with the grid line between the two grid points, for example, (i, j, k) and $(i+1, j, k)$, the two points should be determined as follows:

$$\phi(i, j, k)\phi(i+1, j, k) < 0 . \tag{20}$$

According to the principle of the level set method, the value of the level set function ϕ at (i, j, k) is equal to the signed distance from this point to the interface. Therefore, the position of the monitoring point in the x direction can be determined by using the coordinate value of (i, j, k) and the value of the level set function ϕ at (i, j, k).

3. ANALYTICAL MODEL

An analytical model was previously developed by Ichikawa et al. [11] by considering a mass-spring-damper system to predict the resonance frequency of a cylindrical liquid bridge of diameter, D, and height, H. The model briefly summarized below was used to determine the functional dependence of the resonance frequency on the

liquid bridge dimensions and physical properties. Let the following parameters represent the relevant system parameters: the moving liquid mass, m, damping coefficient, $2mk$, and restoring force (or spring) coefficient, $m\omega_0^2$. The forced external vibration is assumed to be given by $F_0\sin\omega t$, where F_0 is the amplitude of the external force, ω is the angular frequency and t is time. The governing equation is given by,

$$m\ddot{x} + 2mk\dot{x} + m\omega_0^2 x = F_0 \sin \omega t , \tag{21}$$

where x is the displacement of the center of mass of the liquid bridge from the equilibrium position. For $k < \omega_0$, an analytical solution to Eq. (21) is given by,

$$x = C\cdot e^{-kt}\cos\left(\sqrt{\omega_0^2 - k^2}\cdot t + \beta\right) + \frac{1}{\sqrt{\left(\omega_0^2 - \omega^2\right)^2 + 4k^2\omega^2}}\cdot\frac{F_0}{m}\sin\left(\omega t - q\right). \tag{22}$$

where C and β are constants, and q is determined from $\tan q = 2k\omega/(\omega_0^2-\omega^2)$. The second term on the right-hand side is the particular solution and indicates the motion of the liquid bridge responding to the external forced vibration. If $k < \omega_0/\sqrt{2}$, this term has a local maximum at the following angular frequency,

$$\omega = \sqrt{\omega_0^2 - 2k^2} . \tag{23}$$

Equation (23) shows the resonance frequency of the system, ω_R, at which the amplitude of the liquid bridge displacement is expected to be exceptionally large.

To apply these results to the liquid bridge motion, we need to evaluate the values of m, k and ω_0, and thus use the following assumptions.

1) Liquid is a Newtonian fluid and the flow induced within the liquid bridge is laminar.
2) The liquid bridge moves only in the horizontal direction. The shape of the horizontal cross section remains circular and the same at any height of the liquid bridge.
3) Gravity effects are negligible.

Evaluation of m

In the case of a deforming liquid bridge, the moving mass, m, is not the total mass of the liquid between the two disks because of the no-slip condition at the upper and lower disk surfaces. To account for this, a parameter, B, which is a ratio of the moving mass to the total mass of the liquid bridge is introduced. Then, the moving mass of the liquid bridge can be written as

$$m = \frac{\rho\pi D^2 H}{4}\cdot B , \tag{24}$$

where ρ is the liquid density. Possible values of B for three hypothetical situations are shown in Fig. 2.

Evaluation of k (Damping effect)

The value of k represents the damping effect, which is caused by the viscosity of the liquid bridge, μ. Under the assumption of the liquid bridge motion shown in Fig. 2 (c), the value of k is obtained from the following:

$$k = \frac{\pi D^2}{4mH}\mu = \frac{\nu}{H^2}\cdot\frac{1}{B}, \tag{25}$$

where ν ($=\mu/\rho$) is the kinematic viscosity of liquid.

Evaluation of ω_0 (Restoring force)

The last parameter is the restoring force due to surface tension that brings the deformed surface to the equilibrium position given by a straight cylinder in this case. We can calculate the x-direction force from the integral of the pressure difference for the entire free surface of the liquid bridge. By assuming the principal radii

of the surface curvature at any height are the same as those at the mid-height of the liquid bridge, the restoring force parameter is given by,

$$\omega_0 = \frac{4}{H}\sqrt{\frac{\sigma}{D\rho}\cdot\frac{1}{B}}. \tag{26}$$

Evaluation of resonance frequency

By combining Eqs. (22) through (26), the resonance frequency in Hz is given by,

$$f_R = \frac{\omega_R}{2\pi} = \frac{1}{2\pi H}\sqrt{\frac{2}{B}\left(\frac{8\sigma}{D\rho} - \frac{\nu^2}{H^2 B}\right)}. \tag{27}$$

The resonance frequency is predicted to decrease with increasing D, ρ and ν, and to increase with an increase in σ. In practical situations, the second term in the brackets is negligible in comparison with the first term. This is easily found if we calculate the two terms using the thermophysical properties of 5cSt silicone oil. In this situation, equation (27) can be written as,

$$f_R = \frac{2}{\pi H}\sqrt{\frac{\sigma}{D\rho B}}. \tag{28}$$

The resonance frequency would decrease with increases in H, D, ρ and B.

The analytical model was checked against a limited amount of available resonance frequency data obtained in space by Martinez [12] as shown in Table 1.

4. RESULTS AND DISCUSSION

4.1 Numerical simulation results

The present numerical simulations were performed using a mesh 51 x 51 x 51 and the physical properties of 5 cSt silicon oil under normal gravity as shown in Table 2. The initial shape of the liquid bridge is shown in Fig. 3, which is a straight cylinder. Both the liquid bridge and the surrounding air are at rest initially. After the computation is started, the liquid bridge shape first deforms due to gravity and then responds to the small vibrations applied in the horizontal direction. The amplitudes of periodic surface oscillations predicted were determined at different elevations above the bottom of the liquid bridge.

To quantify the response of the liquid bridge surface to small vibrations applied in the horizontal direction, simulations were systematically conducted for a liquid bridge under normal gravity using a 51 x 51 x 51 mesh. The diameter of the liquid bridge was 7.0 mm, and the height was 3.5 mm. The applied vibration frequencies ranged from 3 to 17 Hz, in increments of 2 Hz. The acceleration level in the horizontal direction was kept constant at 18-mg. Three monitoring points on the surface of the liquid bridge were selected at heights of $H/4$, $H/2$, $3H/4$, from the bottom disk. Figures 4 and 5 show the oscillation of the surface for vibration frequencies of 3Hz and 9Hz, respectively. Because of the deformation of the liquid bridge due to gravity, the surface oscillation amplitudes obtained at the three heights are different, and the mid-height of the bridge is the position that gives the largest amplitude among the three monitoring points as shown in Figs. 4 and 5. The tendency of the surface oscillation at heights $H/4$, $H/2$, and $3H/4$ is the same except for the initial period.

The relationship between the surface amplitude at the mid-height and the applied vibration frequency is shown in Fig. 6 for the case of a liquid bridge with the ratio of the minimum diameter of the liquid bridge to the disk diameter (D_{min}/D_{disk}) equal to 0.778. In Fig. 6, an extremely large amplitude can be seen at about 11Hz. The amplitudes at other vibration frequencies are much lower, and they have the same order of magnitude. It is clear that the resonance frequency is at about 11Hz in this set of computations.

4.2 Surface oscillation characteristics under microgravity

To compare the numerically predicted resonance frequency with that of an analytical model described earlier, additional numerical simulations were conducted under zero gravity. In this set of computations, the diameter and height of the liquid bridge were 8.4mm and 4.2mm, respectively, and the applied vibration frequency ranged from 3 to 17Hz. The acceleration level in the horizontal direction was again kept constant at 18-mg, and the mesh used was 51 x 51 x 51.

Figures 7 and 8 show the evolution of the surface position at the mid-height ($H/2$) for vibration frequencies of 3Hz and 9Hz, respectively. The surface of the liquid bridge vibrates periodically due to the horizontal vibration applied, and the amplitude almost reaches a constant value after a few cycles. The surface oscillation amplitude for the vibration frequency of 9Hz is much higher than that predicted for 3Hz. By measurement the amplitudes for the surface of the liquid bridge at every vibration frequency, the relation between the liquid bridge oscillation amplitude and the vibration frequency applied is obtained as shown in Fig. 9. The surface oscillation amplitude remains low at all vibration frequencies except for 9Hz, at which significantly larger amplitude is obtained due to the resonance behavior of the liquid bridge.

4.3 Effects of liquid bridge diameter and height on the resonance frequency

Figure 10 shows the relation between the numerically predicted resonance frequency and the disk diameter for a liquid bridge of H = 3.5mm. The calculations were performed at an acceleration level of 5mg in the absence of gravity. As predicted by the analytical model, Eq. (27) or (28), the resonance frequency decreases with the increasing disk diameter. The predictions of the analytical model are also shown in the figure for several different values of B, B=1 and B = 0.9 (for D = 5.0 mm) or 0.92 (for D = 7.0 and 10.0 mm), where B is the ratio of the moving mass to the total mass of the liquid bridge. In general, due to the no slip condition at the upper and lower disk surfaces, the moving mass is not the total mass of the liquid, thus B can not be equal to 1.0.

For the analytical model, we expected the value of B to fall between 1/2 and 1.0. By comparing the numerical results with the analytical model predictions, it is clear that the analytical predictions with B = 0.9 or 0.92 are closer to the numerical results than those obtained with B=1.0. That means about 90% of the mass of the liquid bridge is induced to move in response to the horizontal vibrations.

Next, the effect of the liquid bridge height on the resonance frequency is investigated. Three different liquid bridge heights were considered while keeping the diameter of the bridge constant at D = 7.0mm and the acceleration at 5mg in the absence of gravity. As shown in Fig. 11, the resonance frequency decreases with the increasing height of the liquid bridge. The resonance frequency varies over the range of 3-11Hz when the height of liquid bridge is changed from 3.5mm to 10.5mm. Both the computational results and the analytical model predictions show the same trend, and they agree closely for different values of the parameter B.

4.4 Effects of physical properties on the resonance frequency

Figure 12 shows the relation between the resonance frequency and density of the liquid bridge calculated for a liquid bridge of 3.5 mm height, 7.0 mm diameter, and an acceleration level of 5mg, in the absence of gravity. The density of the bridge was changed from 700 kg/m^3 to 1200 kg/m^3. It is clear from Fig. 12 that the resonance frequency decreases with the increasing density.

The effect of the liquid density predicted by the numerical model are in close agreement with the analytical model predictions. The best agreement is obtained with B = 0.9 ~ 0.92 rather than B = 1.0 in the analytical model.

4.5 The optimum value of B

In the analytical model, a parameter B was introduced, which is the ratio of the moving mass to the total mass of the liquid bridge. Its value was considered to fall between 1/2 and 1, but would depend on the height of the liquid bridge for a given diameter, or the aspect ratio. From several comparisons of analytical model predictions with the numerical simulations, it is clear that the best value of B is not constant for different aspect ratios of the liquid bridge. The relation between the best value of B and the aspect ratio has been determined and is shown in Fig. 13. Because of the no-slip condition at the upper and lower disk surfaces, as the liquid bridge height is increased, a smaller fraction of the total liquid mass would remain stationary despite the external vibrations. Thus, it is reasonable that the best value of B increases as the aspect ratio is increased, and reaches a constant value almost equal to unity when the aspect ratio is larger than 1.5.

4.6 Effects of liquid bridge height and diameter on the surface oscillation amplitude

Next, the numerical simulation results for the surface oscillation amplitudes are examined in detail. The effect of the liquid bridge height is studied for different vibration frequencies including the resonance frequency. Figure 14 shows the relation between the surface oscillation amplitude and liquid bridge height when the disk diameter is 7.0 mm and the acceleration level is 5 mg. From the curve corresponding to the resonance frequency, it is clear that the surface amplitude increases as the height is increased, especially when the height is large than 7.0 mm. At other vibration frequencies, changing the height does not affect the surface amplitude significantly. Because the resonance frequency of the liquid bridge decreases as the height is increased (the resonance frequency is 10.6Hz, 5.05Hz, 3.36Hz, at H=3.5mm, 7.0mm, and 10.5mm, respectively), the vibration frequency of 9Hz is always far from the resonance frequency and the surface amplitude does not increase with the liquid bridge height. For the vibration frequency of 1.0 Hz, the vibration energy imparted to the liquid bridge is smaller and the surface amplitude remains low regardless of the liquid bridge height.

4.7 Relation between the applied vibration amplitude and surface oscillation amplitude

The relation between the surface oscillation amplitude and applied vibration amplitude is shown in Fig. 15. Both the analytical model predictions with B = 0.9 and numerical simulation results show a linear relation between the applied vibration amplitude and surface amplitude of a liquid bridge with D = 7.0 mm, H = 3.5 mm, at an applied vibration frequency of 5Hz. This vibration frequency is well below the resonance frequency of 10.6Hz. As the applied vibration amplitude is increased from 10 microns to 200 microns while keeping the applied vibration frequency constant at 5Hz, the surface amplitude increases from 2.8 microns to 56 microns. The surface amplitude of the liquid bridge is approximately equal to 0.284 times the vibration amplitude. The analytical model predictions are again seen to be in good agreement with the numerical simulation results.

4.8 Predictions for larger cylindrical bridges

Finally, the surface oscillation of a large diameter liquid bridge for a vibration frequency of 5 Hz and acceleration level of 5 mg under microgravity is predicted as shown in Fig. 16. The liquid bridge diameter is 30.0 mm and the height is 10 mm. From this prediction, the surface amplitude is estimated to be about 100 microns. Another prediction for a vibration frequency of 9 Hz is shown in Fig. 17. The amplitude is smaller as the vibration frequency is further away from the resonance frequency which is predicted by the analytical model to be 1.706 Hz, if B = 1.0 is used. The relation between the numerically predicted surface amplitude and applied

vibration frequency is shown in Fig. 18. The resonance frequency is predicted to be near 1.7 Hz, which is close to the analytically predicted value.

5. CONCLUSIONS

The vibration-induced oscillation of an isothermal liquid bridge has been investigated numerically. A three-dimensional DNS analysis of the liquid bridge was conducted using a level set approach to capture small surface oscillations for a non-axisymmetric liquid bridge induced by a horizontal vibration of different frequencies and amplitudes. An analytical model developed earlier based on a mass-spring-damper analogy was also used to compare with the numerical simulation predictions. Analytical expressions were derived for the surface oscillation amplitude and resonance frequency for a liquid bridge with the shape of a straight cylinder. From this work, the following conclusions can be drawn.

1. Three-dimensional oscillatory behavior of a liquid bridge could be predicted by the present numerical model, even for the case of a large density ratio between the liquid and surrounding gas. The level set approach can be used to capture micro-scale displacement of the free surface even though relatively coarse grids are used for simulation.
2. The existence of a resonance frequency, at which the oscillation amplitude of the liquid bridge increases significantly, was clearly predicted both analytically and numerically. The analytical model predictions and numerical simulation results were consistent with one another.
3. Numerical simulations have shown that the resonance frequency decreases with increases in height, diameter and density of the liquid bridge, but increases with surface tension. These predictions for the parametric dependence were consistent with the analytical model predictions.
4. The surface oscillation amplitude of the liquid bridge increases linearly with the applied vibration amplitude at non-resonance frequencies.
5. A comparison of the numerical results with the analytical model predictions showed that about 90% of the total mass of the liquid bridge would move in response to the horizontal vibrations. This fraction is predicted to increase with the liquid bridge height but decrease with the diameter.
6. The numerical simulation model can predict the vibration-induced oscillation of deformed liquid bridges under both normal gravity and microgravity, while the analytical model is applicable to liquid bridges with a straight cylindrical shape that are obtained only under microgravity.

ACKNOWLEDGMENTS

The authors would like to thank the Japan Aerospace Exploration Agency and Canadian Space Agency for financially supporting this IAO project.

REFERENCES

1. A. Pline, T. Jacobson, Y. Kamotani and S. Ostrach: Surface Tension Driven Convection Experiment, AIAA Paper 93-4312 (1993).
2. A. Hirata, S. Nishizawa, N. Imaishi, S. Yasuhiro, S. Yoda and K. Kawasaki: Oscillatory Marangoni Convection in a Liquid Bridge under Microgravity by Utilizing TR-IA Sounding Rocket, J. Jpn. Soc. Microgravity Appl., 10-4, 241 (1993).

3. K. Nishino, T. Yamasaki and M. Takami: Three-Dimensional Flow Visualization and Measurement of Suspended Liquid Bridge, J. Jpn. Soc. Microgravity Appl., 12-4, 205 (1995).
4. S. Nakamura, T. Hibiya, K. Kakimoto, N. Imaishi, S. Nishizawa, A. Hirata, K. Mukai, S. Yoda, and T. Morita: Temperature Fluctuations of the Marangoni Flow in a Liquid Bridge of Molten Silicon under Microgravity on Board the TR-IA-4 Rocket, J. Crystal Growth, 186, 85 (1998).
5. L. Carotenuto, D. Castagnolo, C. Albanese and R. Monti: Instability of Thermocapillary Convection in Liquid Bridges, Phys. Fluids, 10-3, 555 (1998).
6. V. M. Shevtsova and J.C. Legros: Oscillatory Convective Motion in Deformed Liquid Bridges, Phys. of Fluids, 10-7, 1621 (1998).
7. Q. S. Chen and W. R. Hu: Influence of Liquid Bridge Volume on Instability of Floating Half Zone Convection, Int. J. Heat Mass Transfer, 41, 825 (1998).
8. S. Osher and J. A. Sethian: Fronts Propagating with Curvature-Dependent Speed: Algorithms Based on Hamilton-Jacobi Formulations, J. Comput. Phys. 79, 49 (1988).
9. M. Sussman, P. Smereka, and S. Osher: A Level Set Approach for Computing Solutions to Incompressible Two-Phase Flow, J. Comput. Phys. 114, 146 (1994).
10. J. U. Brackbill, D. B. Kothe, and C. Zemach: A Continuum Method for Modeling Surface Tension, J. Comput. Phys. 100(2), 335 (1992).
11. N. Ichikawa, M. Kawaji and M. Misawa: Resonance Behavior of a Liquid Bridge Caused by Horizontal Vibrations. Journal of the Japan Society of Microgravity Applications, Vol. 20, No. 4, pp. 292-300 (2003).
12. I. Martinez: Stability of Liquid Bridges, Results of SL-D1 Experiment, Acta Astronautica, 15, 449 (1987).

Table 1. Comparison of analytical model predictions with SL-D1 experimental results by Martinez [12]

Experimental Run	Aspect Ratio (H/D)	Experimental Resonance Frequency (Hz)	Resonance frequency predicted by model (Hz) B=1.0
SL-D1-#2	2.71	0.18	0.17
SL-D1-#3	2.71	0.19	0.17
SL-D1-#4	2.86	0.17	0.16
SL-D1-#5	2.71	0.17	0.17
SL-D1-#6	2.57	0.19	0.18

Table 2. Physical properties for 5 cSt silicon oil

		5 cSt silicone oil	Air
Density [kg/m^3]	ρ	915	1.226
Viscosity [kg/ms]	μ	4.575×10^{-3}	1.78×10^{-5}
Surface tension [N/m]	σ	1.97×10^{-2}	—
Gravity [m/s^2]	g	9.81	

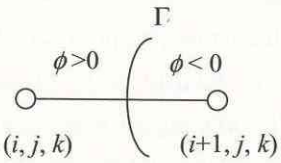

Fig. 1 An interface intersecting with a grid at x-y plane

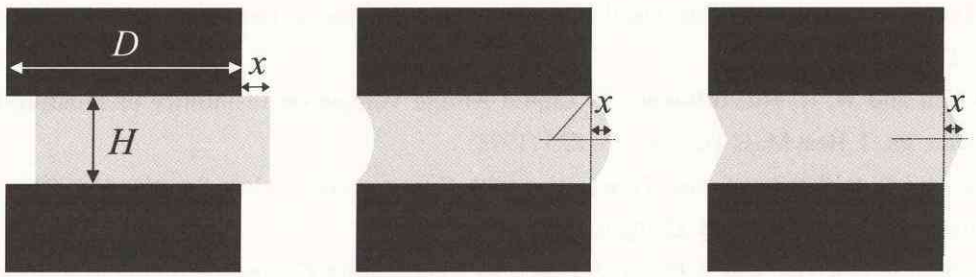

(a) whole liquid moving (B = 1) (b) curved interface (1/2 < B < 1) (c) triangular interface (B = ½)

Fig. 2 Models of a liquid bridge movement and values of B

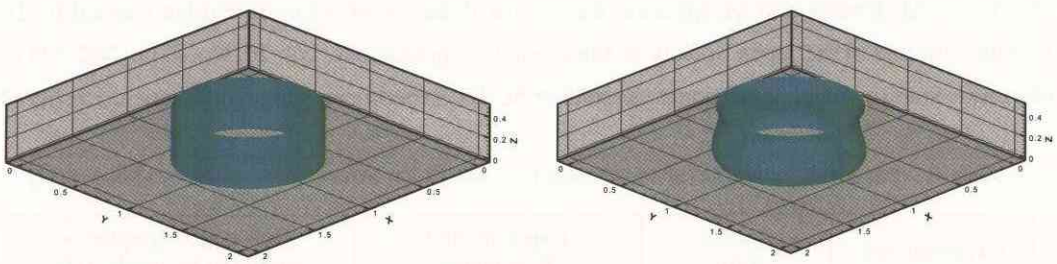

Fig. 3 Deformation of an initially cylindrical liquid bridge due to gravity

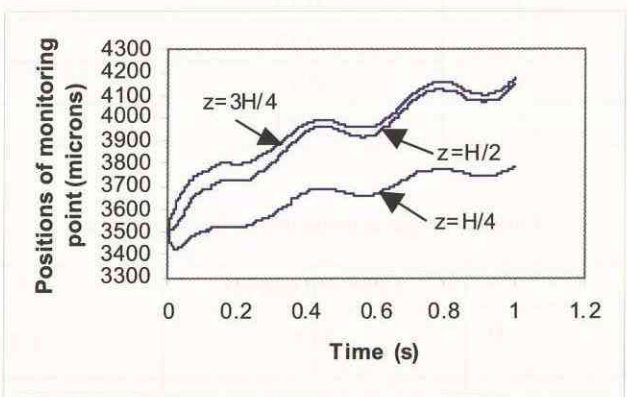

Fig. 4 Evolution of the surface positions at three different heights for a liquid bridge of D = 7.0 mm, H = 3.5 mm for an applied vibration frequency of 3Hz and acceleration level of 18 mg

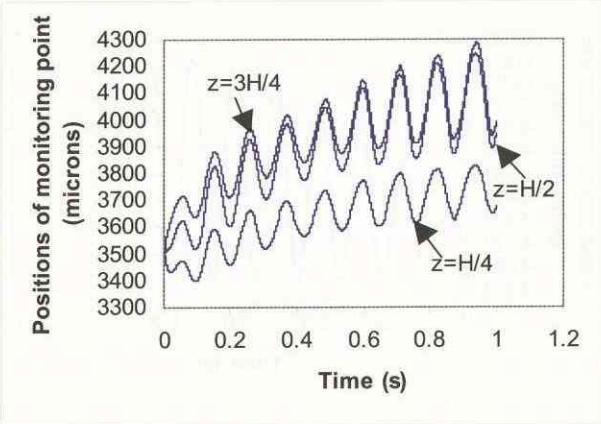

Fig. 5 Evolution of the surface positions at three different heights for a liquid bridge of D = 7.0 mm, H = 3.5 mm for an applied vibration frequency of 9Hz and acceleration level of 18 mg

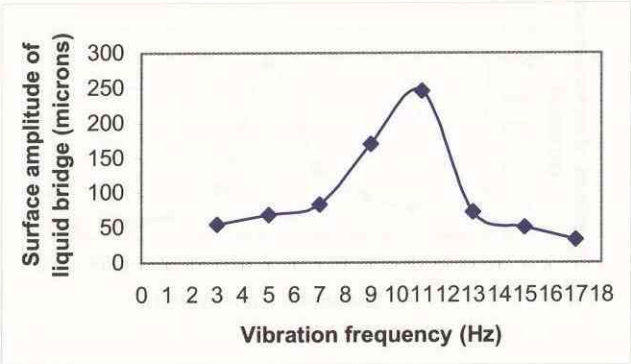

Fig. 6 Relation between surface oscillation amplitudes and applied vibration frequencies for a liquid bridge of D = 7.0 mm, H = 3.5 mm and the minimum diameter of the liquid bridge to the disk diameter (D_{min}/D_{disk}) = 0.778 under normal gravity

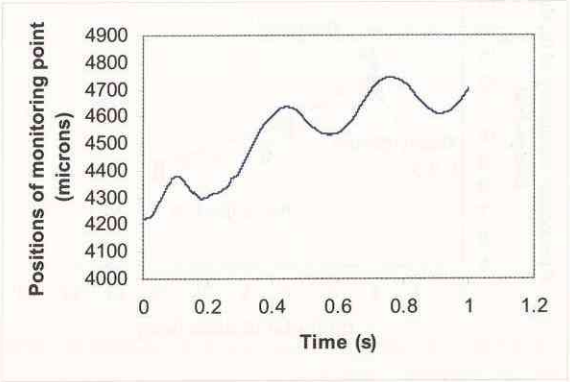

Fig. 7 Evolution of the surface position at mid-height for a liquid bridge of D = 8.4 mm and H = 4.2 mm at an applied vibration frequency of 3Hz and acceleration level of 18 mg

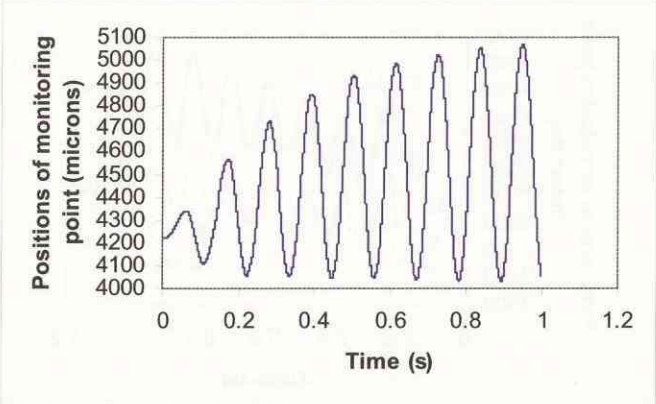

Fig. 8 Evolution of the surface position at mid-height for a liquid bridge of D = 8.4 mm and H = 4.2 mm at an applied vibration frequency of 9 Hz and acceleration level of 18 mg

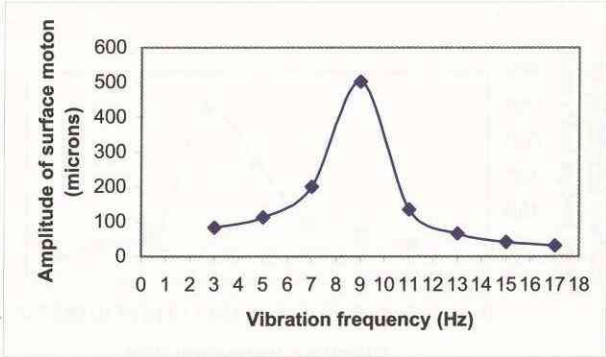

Fig.9 Relation between surface amplitude and vibration frequency for a liquid bridge of D = 8.4 mm and H = 4.2 mm

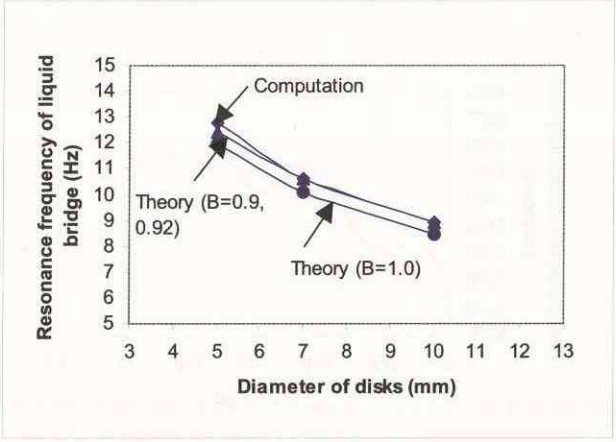

Fig. 10 Variation of resonance frequency with disk diameter for a liquid bridge of H = 3.5 mm

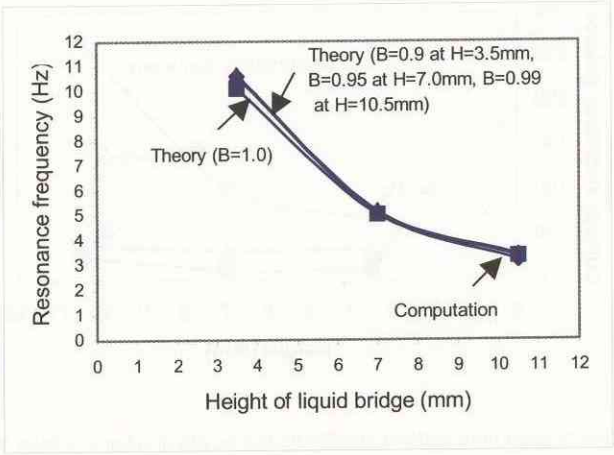

Fig. 11 Effect of liquid bridge height on resonance frequency for a liquid bridge of D = 7.0 mm

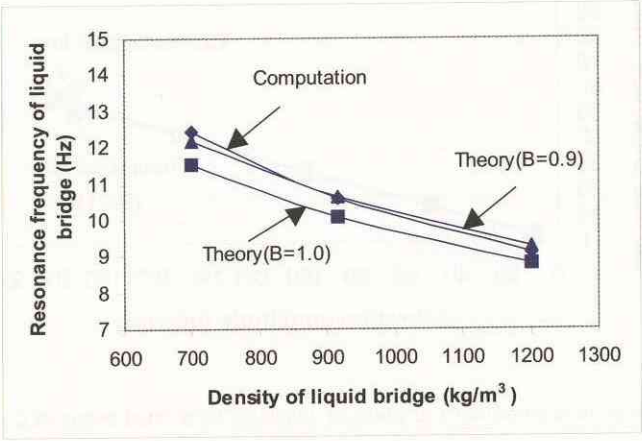

Fig. 12 Effect of density on the resonance frequency of a liquid bridge of D= 7.0mm and H = 3.5mm

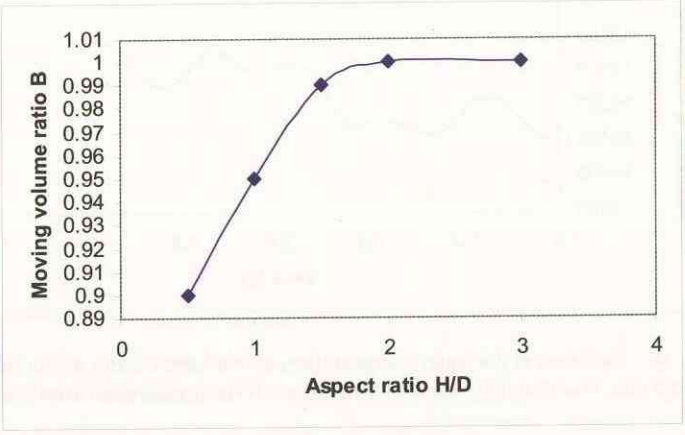

Fig. 13 Relation between moving volume ratio, B, and aspect ratio for a liquid bridge of D = 7.0 mm and H = 3.5 mm

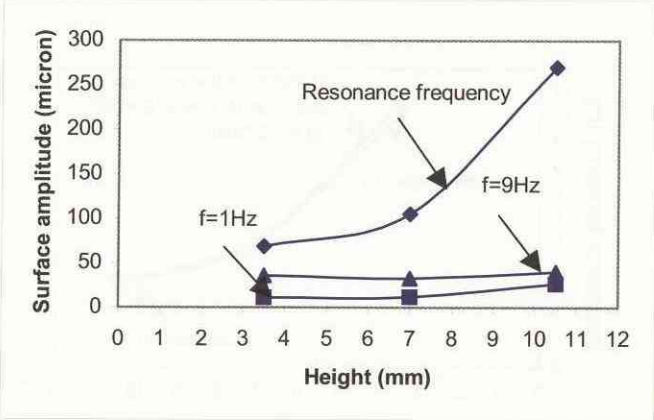

Fig. 14 Relation between the surface amplitude and height of a liquid bridge for D = 7.0 mm

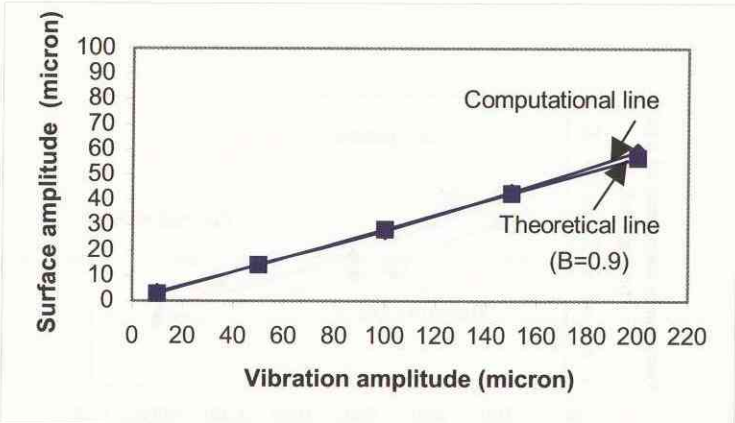

Fig. 15 Relation between surface amplitude and vibration amplitude for a liquid bridge of D = 7.0 mm and H = 3.5 mm

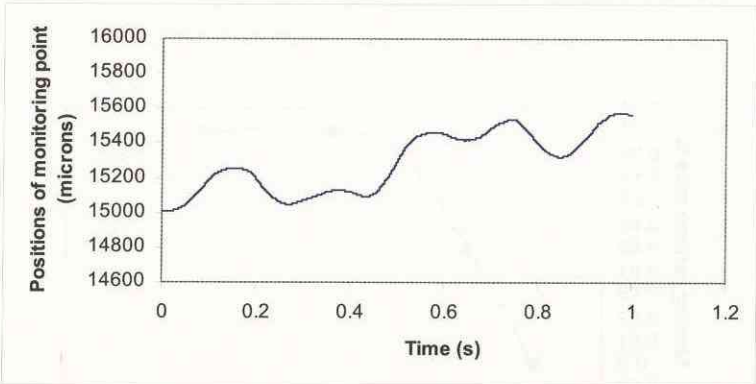

Fig. 16 Evolution of the liquid bridge surface at mid-height under microgravity
(D = 30.0 mm, H = 10.0 mm, vibration frequency = 5 Hz, acceleration level = 5.0 mg)

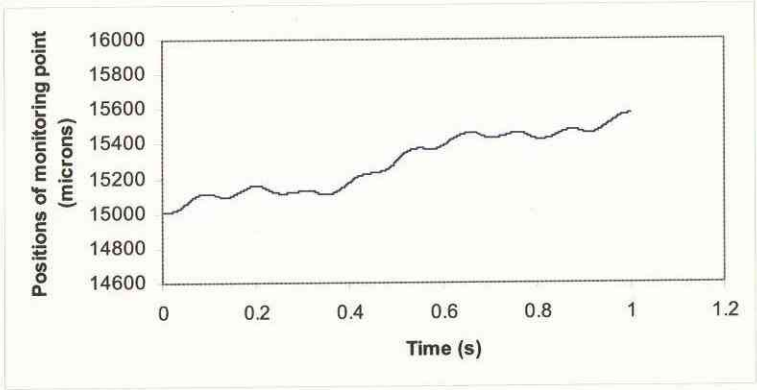

Fig. 17 Evolution of the liquid bridge surface at mid-height under microgravity (D = 30.0 mm, H = 10.0 mm, vibration frequency = 9 Hz, acceleration level = 5.0 mg)

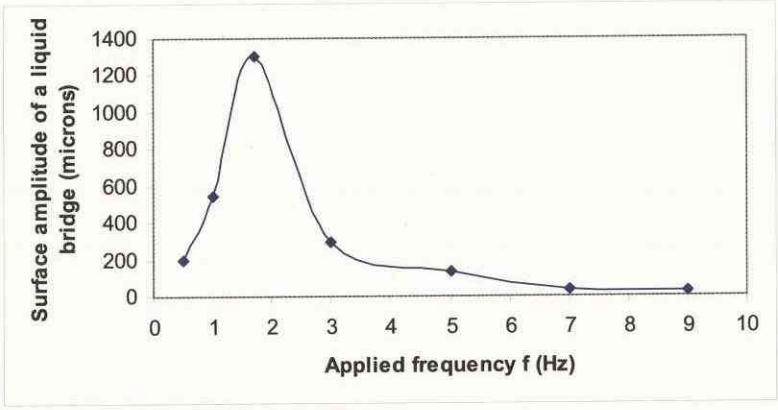

Fig. 18 Relation between the surface amplitude of a liquid bridge and applied vibration frequency under microgravity (D = 30.0 mm, H = 10.0 mm, Acceleration level = 5.0 mg; Computational resonance frequency = 1.7Hz, analytical resonance frequency=1.706Hz)